

# Dopamine receptor subtypes modulate olfactory bulb $\gamma$ -aminobutyric acid type A receptors

INA BRÜNIG\*, MICHAEL SOMMER, HANNS HATT, AND JOACHIM BORMANN†

Ruhr-Universität Bochum, Lehrstuhl für Zellphysiologie, D-44780 Bochum, Germany

Edited by Erminio Costa, University of Illinois, Chicago, IL, and approved December 22, 1998 (received for review July 29, 1998)

**ABSTRACT** The  $\gamma$ -aminobutyric acid type A (GABA<sub>A</sub>) receptor is the predominant Cl<sup>-</sup> channel protein mediating inhibition in the olfactory bulb and elsewhere in the mammalian brain. The olfactory bulb is rich in neurons containing both GABA and dopamine. Dopamine D1 and D2 receptors are also highly expressed in this brain region with a distinct and complementary distribution pattern. This distribution suggests that dopamine may control the GABAergic inhibitory processing of odor signals, possibly via different signal-transduction mechanisms. We have observed that GABA<sub>A</sub> receptors in the rat olfactory bulb are differentially modulated by dopamine in a cell-specific manner. Dopamine reduced the currents through GABA-gated Cl<sup>-</sup> channels in the interneurons, presumably granule cells. This action was mediated via D1 receptors and involved phosphorylation of GABA<sub>A</sub> receptors by protein kinase A. Enhancement of GABA responses via activation of D2 dopamine receptors and phosphorylation of GABA<sub>A</sub> receptors by protein kinase C was observed in mitral/tufted cells. Decreasing or increasing the binding affinity for GABA appears to underlie the modulatory effects of dopamine via distinct receptor subtypes. This dual action of dopamine on inhibitory GABA<sub>A</sub> receptor function in the rat olfactory bulb could be instrumental in odor detection and discrimination, olfactory learning, and ultimately odotopic memory formation.

$\gamma$ -Aminobutyric acid (GABA) is a major inhibitory neurotransmitter in the mammalian central nervous system (1). Three types of pharmacologically and physiologically distinct GABA receptors have been described. Activation of bicuculline-sensitive GABA<sub>A</sub> receptors causes the opening of integral ion channels selectively permeable to Cl<sup>-</sup> (2–5). The baclofen-sensitive GABA<sub>B</sub> receptors couple to either Ca<sup>2+</sup> or K<sup>+</sup> channels via G proteins (3, 6, 7). The recently described GABA<sub>C</sub> receptors are Cl<sup>-</sup> channels insensitive to both bicuculline and baclofen (8–11). Several different subunits have been identified for the mammalian GABA<sub>A</sub> receptor, including six  $\alpha$  subunits, three  $\beta$  subunits, four  $\gamma$  subunits, and one  $\delta$  subunit (5, 12, 13). Each subunit consists of four membrane-spanning regions (M1–M4) and a cytoplasmic loop between M3 and M4 (14). The intracellular loop of the  $\beta$ -subunit contains consensus sites for phosphorylation by protein kinases (14–16). Protein kinase A (PKA) and C (PKC) are both involved with second-messenger pathways that can modulate the function of GABA<sub>A</sub> receptors (15–19).

In the present study, we investigated the modulation of GABA<sub>A</sub> receptors in the rat olfactory bulb. This brain region is rich in neurons that contain both GABA and dopamine (20, 21) as well as high densities of dopamine receptors (22, 23). The distinct and complementary distribution of D1 and D2 receptor subtypes suggests that dopamine may control the GABAergic inhibitory processing of odor signals, possibly via

different signal-transduction mechanisms. Using patch-clamp techniques, we have identified two distinct pathways by which dopamine receptors can either up- or down-modulate GABAergic function in the rat olfactory bulb. These pathways involve the stimulation of second-messenger systems and subsequent phosphorylation of GABA<sub>A</sub> receptors by PKA or PKC.

## MATERIALS AND METHODS

**Cell Culture.** Primary cultures of rat olfactory-bulb neurons were prepared from animals at embryonic day 19. The tissue was trypsinized (0.1%), and cells were plated on poly-L-lysine- and laminin-coated (Sigma) plastic dishes. The growth medium was Eagle's basal medium (GIBCO) supplemented with insulin (6.5  $\mu$ M, Sigma), glutamine (2 mM), glucose (20 mM), and 10% fetal calf serum (GIBCO). Cytosine arabinofuranoside (10  $\mu$ M, Sigma) was added after 2 days to inhibit the growth of nonneuronal cells. Interneurons and mitral/tufted (M/T) cells were visually identified (24, 25) and recorded from after 5–8 days in culture. Because granule cells represent the majority of interneurons in the olfactory bulb, the interneurons studied here were probably granule cells (26).

**Electrophysiology.** The preparation was viewed with phase-contrast optics at  $\times 320$  magnification and continuously superfused (1 ml/min) at room temperature (21–25°C). The extracellular bath solution contained (in mM): 137 NaCl, 5.4 KCl, 1.8 CaCl<sub>2</sub>, 1 MgCl<sub>2</sub>, and 5 Hepes (pH 7.4). Whole-cell currents were recorded with the patch-clamp technique (27) at  $-60$  mV membrane potential using an EPC-7 amplifier (List Electronics, Darmstadt, Germany). Pipettes were made from borosilicate glass (Hilgenberg, Malsfeld, Germany) and filled with a solution containing (in mM): 120 CsCl, 20 tetraethylammonium chloride, 1 CaCl<sub>2</sub>, 2 MgCl<sub>2</sub>, 11 EGTA, and 10 Hepes (pH 7.2). Pipette resistance was 5–7 M $\Omega$ . We routinely corrected for the liquid junction potential (2). The series resistance of the pipettes (12–20 M $\Omega$ ) was compensated by up to 80%.

Extracellular drugs were dissolved in the bath solution and rapidly applied to cells. The fast-application system consisted of an array of pressure pipettes in conjunction with a suction pipe on the opposite side of the cell. With this device, it was possible to change the solution in the vicinity of a whole cell within 50–100 ms. We waited 2 minutes after patch breakthrough before applying the first GABA pulse to allow for complete intracellular Cl<sup>-</sup> equilibration. Phorbol 12-myristate 13-acetate (PMA) was prepared in dimethyl sulfoxide as 1 mM

This paper was submitted directly (Track II) to the *Proceedings* office. Abbreviations: GABA,  $\gamma$ -aminobutyric acid; GABA<sub>A</sub> receptor, GABA type A receptor; PKA, cAMP-dependent protein kinase; PKC, protein kinase C; SKF-38393, (+)-1-phenyl-2,3,4,5-tetrahydro(1H)-3-benzazepine-7,8-diol hydrochloride; PMA, phorbol 12-myristate 13-acetate; M/T cells, mitral/tufted cells.

\*Present address: Institute of Pharmacology, University of Zürich, Winterthurerstrasse 190, CH-8057 Zürich, Switzerland.

†To whom reprint requests should be addressed at: Ruhr-Universität Bochum, Lehrstuhl für Zellphysiologie, ND4/132, D-44780 Bochum, Germany. e-mail: Joachim.Bormann@ruhr-uni-bochum.de.

The publication costs of this article were defrayed in part by page charge payment. This article must therefore be hereby marked "advertisement" in accordance with 18 U.S.C. §1734 solely to indicate this fact.

PNAS is available online at www.pnas.org.

stock solution and tamoxifen was dissolved at 10 mM in methanol and added to the intracellular solution. All drugs used in electrophysiological experiments were purchased from Sigma, except PMA, (+)-1-phenyl-2,3,4,5-tetrahydro(1H)-3-benzazepine-7,8-diol hydrochloride (SKF-38393), guanosine 5'-[ $\gamma$ -thio]triphosphate (GTP[ $\gamma$ S]) and (-)-bicuculline methiodide (Research Biochemicals, Natick, MA).

**Data Analysis.** Time-dependent changes of GABA-induced currents were assessed by normalizing the peak amplitudes ( $I$ ) to the first GABA response at  $t = 2$  min ( $I_C$ ). Effects of extra- and intracellular drugs were compared with control after 14 or 12 minutes of recording, respectively.

Dose-response curves were constructed for control cells that yielded stable GABA responses under our conditions. Currents ( $I$ ) were normalized relative to the value obtained with 1 mM GABA ( $I_{\max}$ ) and fitted with the equation:

$$\frac{I}{I_{\max}} = \frac{c^n}{c^n + EC_{50}^n} \quad [1]$$

where  $I/I_{\max}$  is the normalized current,  $c$  is GABA concentration,  $EC_{50}$  is the GABA concentration giving 50% of the maximal response, and  $n$  is the Hill coefficient.

The dose-response behavior of the phosphorylated GABA receptors could not be measured directly because the currents typically did not reach steady state after 14 min of recording. We therefore devised an alternative strategy to detect changes in  $EC_{50}$  and  $I_{\max}$ . Two GABA (5  $\mu$ M) responses were selected, ( $I_C = 2$  min;  $I = 14$  min), before a saturating GABA response was elicited ( $I_{1mM}$ ). Using an initial  $EC_{50}$  of 5  $\mu$ M and a Hill coefficient of  $n = 1.5$  (see *Results*), the  $EC_{50}$  is operationally determined at  $t = 14$  min as:

$$EC_{50} = 5 \mu M \sqrt[1.5]{\frac{I_{1mM}}{I} - 1} \quad [2]$$

Likewise, because the initial  $I_{\max} = 2I_C$ , i.e., twice the current evoked by 5  $\mu$ M GABA ( $EC_{50}$ ), the relative maximal current,  $I_{\max}^R$ , at  $t = 14$  min is given by the ratio:

$$I_{\max}^R = \frac{I_{1mM}}{2I_C} \quad [3]$$

We validated this approach by applying the procedures to a set of control cells. There was no significant deviation from the outcome of conventional dose-response experiments (see *Results*).

Results are expressed and illustrated as means  $\pm$  SEM, calculated for  $n$  cells. Statistical analysis was performed by using Student's  $t$  test.

## RESULTS

### Differential Modulation of GABA<sub>A</sub> Receptors by Dopamine.

In response to externally applied GABA (5  $\mu$ M), olfactory-bulb neurons displayed large inward currents that were completely blocked by 100  $\mu$ M bicuculline (Fig. 1A), indicating that the underlying receptors were of the GABA<sub>A</sub> type (3, 11). The  $EC_{50}$  values for GABA were  $4.7 \pm 1.7$   $\mu$ M (six granule cells) and  $5.1 \pm 2.2$   $\mu$ M (five M/T cells) (Fig. 1B). The Hill coefficients obtained in these experiments were  $1.5 \pm 0.1$  and  $1.2 \pm 0.1$  for granule and M/T cells, respectively. Thus the GABA<sub>A</sub> receptors present in the two major types of rat olfactory-bulb neurons do not differ significantly in their activation properties.

The peak-current amplitude remained stable even after long periods of recording (Fig. 1C and F). This is illustrated for a granule cell (Fig. 1C) with seven consecutive GABA responses recorded at 2-min intervals. The average ratio  $I/I_C$  of the peak amplitudes measured at 12 min ( $I$ ) and 2 min ( $I_C$ ) after

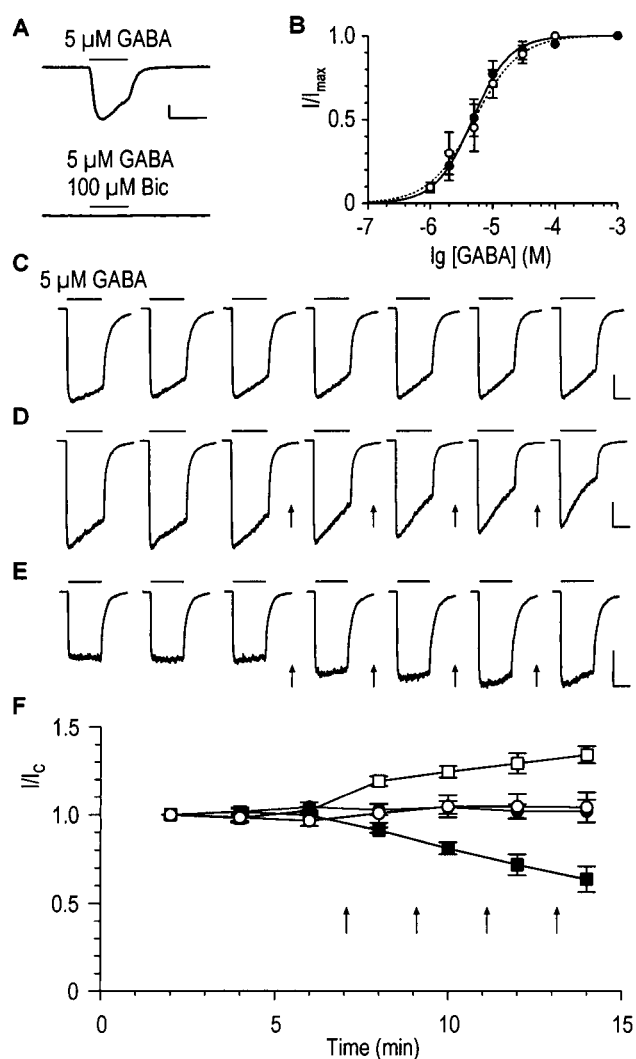


FIG. 1. Dopamine-mediated reduction and enhancement of GABA-induced membrane currents in granule cells and M/T cells of rat olfactory bulb (respectively). Horizontal and vertical scales correspond to 5 s and 500 pA, respectively. (A) GABA-induced whole-cell currents were completely blocked by 100  $\mu$ M bicuculline (Bic). (B) Dose-response curves of GABA-induced peak currents of granule cells (filled symbols) and M/T cells (open symbols). The  $EC_{50}$  was  $4.7 \pm 1.7$   $\mu$ M and the Hill coefficient was  $n = 1.5 \pm 0.1$  for granule cells ( $n = 6$ , solid line). For M/T cells, the values obtained from the fit are  $EC_{50} = 5.1 \pm 2.2$   $\mu$ M and  $n = 1.2 \pm 0.1$  ( $n = 5$ , dashed line). (C–E) Time dependence of GABA-induced membrane currents. (C) Stability of control peak-currents during 14 min of recording illustrated for a granule cell. A moderate acceleration of the speed of desensitization was observed in this and in most other cells. (D) Decrease of control GABA responses in a granule cell after repeated dopamine application (50  $\mu$ M, 30s, arrows). (E) Increase of GABA-induced currents in a M/T cell. (F) Time-dependent changes of normalized GABA responses in control cells (23 granule cells, ●; 6 M/T cells, ○) and dopamine experiments (6 granule cells, ■; 4 M/T cells, □).

commencement of the whole-cell recording was  $1.02 \pm 0.04$  (23 cells). Likewise, an average ratio of  $1.05 \pm 0.07$  was obtained for M/T cells ( $n = 6$ ). The stability of GABA-induced currents was a characteristic feature of olfactory-bulb neurons, and the time course was virtually identical for the two cell types studied here (Fig. 1F).

The presence of different dopamine receptor subtypes on granule and M/T cells with possibly different transduction mechanisms prompted us to investigate the effect of dopamine on olfactory bulb GABA<sub>A</sub> receptors. When dopamine was

applied (50  $\mu$ M; 30 s) to granule cells between successive GABA applications (Fig. 1 *D* and *F*, arrows), the GABA-induced current gradually decreased ( $I/I_C = 0.64 \pm 0.07$ ;  $n = 6$  cells). Using the same protocol, the GABA responses were enhanced by dopamine in M/T cells ( $I/I_C = 1.34 \pm 0.05$ ;  $n = 4$  cells; Fig. 1 *E* and *F*). Dopamine alone did not induce any membrane current (data not shown). Thus, dopamine can either up- or down-modulate the function of GABA<sub>A</sub> receptors in olfactory-bulb neurons.

**D1 Receptors Reduce GABA Responses in Granule Cells via the PKA Cascade.** To characterize the dopamine receptor subtype mediating the decrease of GABA-induced currents in granule cells, we tested SKF-38393, a specific agonist for dopamine D1 receptors. With 50  $\mu$ M SKF-38393, a decrease similar to that induced by dopamine was observed ( $I/I_C = 0.44 \pm 0.06$ ;  $n = 5$  cells; Fig. 2*A*). When a PKA-inhibitory peptide (5  $\mu$ g/ml) was included in the pipette solution, the GABA response was no longer reduced by SKF-38393 ( $I/I_C = 1.01 \pm 0.03$ ;  $n = 5$  cells; Fig. 2*B*). The D2 agonist bromocryptine (50  $\mu$ M) was inactive on granule cells (Fig. 2*G*). Thus, down-modulation of GABA-induced Cl<sup>-</sup> currents in olfactory-bulb granule cells following D1 receptor activation may involve phosphorylation of GABA<sub>A</sub> receptors by PKA.

Evidence for a dopamine-mediated phosphorylation of GABA<sub>A</sub> receptors in granule cells was obtained by including cAMP (100  $\mu$ M) in the pipette. Again, the GABA-induced currents decreased to  $I/I_C = 0.40 \pm 0.05$  ( $n = 15$  cells; Fig. 2*C*), an effect not seen when PKA-inhibitory peptide was also present in the pipette (Fig. 2*G*). Given that phosphorylation by PKA decreases the function of GABA<sub>A</sub> receptors, dephosphorylation should have the opposite effect. Fig. 2*D* shows that inclusion of alkaline phosphatase (224 units/ml) in the pipette enhanced the amplitude of the GABA responses ( $I/I_C = 1.78 \pm 0.11$ ;  $n = 4$  cells).

The intracellular modulation of granule cell GABA<sub>A</sub> receptors reported here involves a G protein. Decrease of GABA-induced currents was observed with both the nonhydrolyzable GTP analogue GTP[ $\gamma$ S] (100  $\mu$ M;  $I/I_C = 0.66 \pm 0.11$ ;  $n = 6$  cells; Fig. 2*E*) and with cholera toxin (1  $\mu$ g/ml;  $I/I_C = 0.62 \pm 0.07$ ;  $n = 4$  cells; Fig. 2*F*), which suggests that a G<sub>s</sub> protein mediates the coupling between D1 receptors and adenylate cyclase. PMA (100 nM) was inactive ( $I/I_C = 0.92 \pm 0.04$ ;  $n = 8$  cells; Fig. 2*G*), indicating that PKC does not modulate the GABA<sub>A</sub> receptors in granule cells. Our findings are summarized in a model in which dopamine D1 receptors can elevate the level of cAMP by activating adenylate cyclase via a G<sub>s</sub> protein (Fig. 2*H*). As a consequence, PKA phosphorylation decreases the currents through GABA<sub>A</sub>-receptor channels.

**Up-Modulation of GABA Receptors in M/T Cells Involves D2 Receptors and PKC.** The facilitation of GABA responses seen with dopamine in M/T cells was caused by activation of D2 receptors. As shown in Fig. 3*A*, the potentiating effect of dopamine on GABA-induced currents was mimicked by bromocryptine (50  $\mu$ M;  $I/I_C = 1.60 \pm 0.31$ ;  $n = 4$  cells), a D2-receptor agonist. Involvement of PKC in this effect was supported by the finding that the phorbol ester PMA (100 nM), an activator of PKC, also increased the GABA responses when it was included in the pipette ( $I/I_C = 1.63 \pm 0.15$ ;  $n = 11$  cells; Fig. 3*B*). GABA-activated currents decreased on intracellular administration of the PKC inhibitor tamoxifen (50  $\mu$ M;  $I/I_C = 0.63 \pm 0.06$ ;  $n = 4$  cells; Fig. 3*C*). PKA was not involved, as intracellular cAMP (100  $\mu$ M) did not modulate the GABA responses in M/T cells ( $I/I_C = 1.07 \pm 0.05$ ;  $n = 9$  cells; Fig. 3*D*). The intra- and extracellular pharmacology of the dopamine-mediated facilitation of M/T-cell GABA receptors (Fig. 3*D*) is consistent with a model in which dopamine D2 receptors can elevate the level of intracellular diacylglycerol by activating phospholipase C, presumably via a G protein (Fig. 3*E*). As a consequence, PKC phosphorylation increases the Cl<sup>-</sup> current

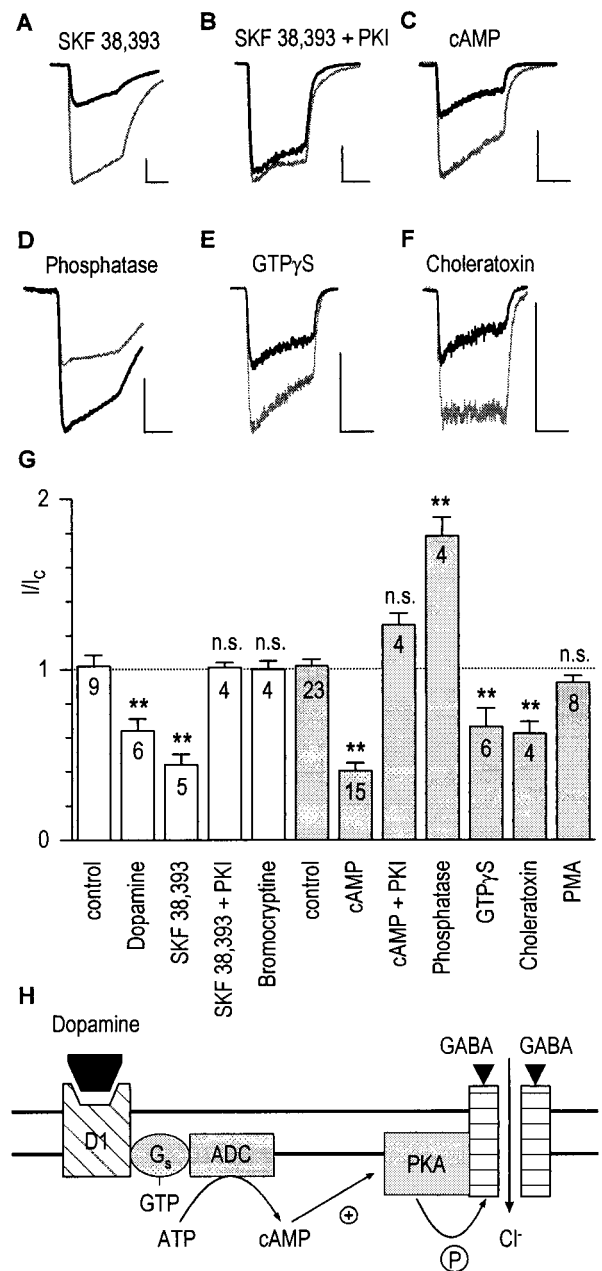


**Fig. 2.** Dopamine D1 receptors mediate down-modulation of GABA<sub>A</sub> receptors via phosphorylation by PKA in granule cells. (*A*) SKF-38393 (50  $\mu$ M; see Fig. 1 for protocol) decreased the GABA control response (light trace) to 34% after 14 min of recording (dark trace). Horizontal and vertical scales in this figure correspond to 5 s and 500 pA, respectively. (*B*) The effect of SKF-38393 was abolished when PKA-inhibitory peptide (5  $\mu$ g/ml) was included in the pipette. (*C*) Intracellular cAMP (100  $\mu$ M) also decreased GABA-induced currents ( $I/I_C = 0.65$ ). (*D*) Potentiation of the GABA response to 186% of control by intracellular phosphatase (224 units/ml). (*E–F*) Decrease of currents by 100  $\mu$ M GTP[ $\gamma$ S] ( $I/I_C = 0.56$ ) and 1  $\mu$ M cholera toxin ( $I/I_C = 0.55$ ). (*G*) Modulatory effects of extra- and intracellular drugs (open and shaded columns, respectively). The dashed line indicates the no-effect level. Statistical differences from control experiments are represented by asterisks (\*\*,  $P \leq 0.01$ ,  $n$  cells). (*H*) Model illustrating the sequence of events for the decrease of GABA-induced currents: Binding of dopamine to D1 receptors leads to activation of adenylate cyclase (ADC), production of cAMP, and eventually phosphorylation of GABA<sub>A</sub> receptors by PKA.

through GABA<sub>A</sub> receptors and thereby increases the inhibitory action of GABA.

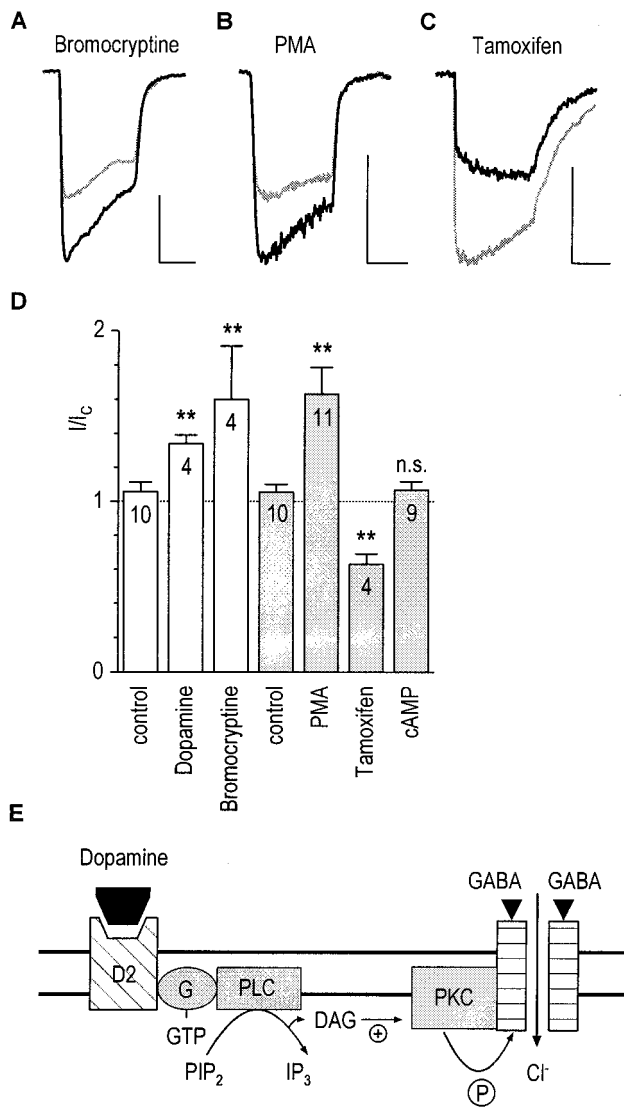


**Fig. 3.** Dopamine D2 receptors mediate up-modulation of GABA<sub>A</sub> receptors in M/T cells via phosphorylation by PKC. (A) Bromocryptine (50  $\mu$ M; see Fig. 1 for protocol) increased the control GABA response (light trace) to 150% (dark trace). Horizontal and vertical scales in this figure correspond to 5 s and 500 pA, respectively. (B) Intracellular application of 100 nM PMA also increased the GABA-induced current ( $I/I_C = 1.53$ ). (C) Decrease of GABA response on including 50  $\mu$ M tamoxifen in the pipette ( $I/I_C = 0.57$ ). (D) Modulatory effects of extra- and intracellular drugs (open and shaded columns, respectively). The dashed line indicates the no-effect level. \*\*,  $P \leq 0.01$ ; \*,  $P \leq 0.05$ ; n cells. (E) Model illustrating the sequence of events for the increase of GABA-induced currents: Binding of dopamine to D2 receptors leads to activation of phospholipase C (PLC), production of diacylglycerol (DAG), and eventually phosphorylation of GABA<sub>A</sub> receptors by PKC.

**Mechanism of GABA<sub>A</sub> Receptor Modulation by PKA and PKC.** Given that GABA<sub>A</sub> receptor function is decreased or enhanced by phosphorylation, we tested whether the observed changes in the GABA response amplitudes are purely time-dependent or if repetitive application of GABA is required. We tackled this question by determining the cAMP-induced run-down in granule cells from two single GABA applications given at  $t = 2$  and 14 min. The ratio  $I/I_C$  was  $0.42 \pm 0.03$  ( $n = 4$  cells) compared with the value of  $0.34 \pm 0.09$  ( $n = 7$  cells) obtained with standard repetitive GABA application. The two results are not statistically different. Similar findings were obtained for the up-modulation of GABA<sub>A</sub> receptors in M/T

cells by PMA, indicating that use-dependent effects cannot account for the modulation of GABA<sub>A</sub> receptors by either PKA or PKC.

A moderate increase of desensitization was observed in most cells, but it was independent of the experimental condition, such as the application of dopamine or of other extracellular or intracellular drugs. Increase of desensitization was even observed in control cells (Fig. 1C), indicating that it cannot account for the protein kinase effects on the amplitude of GABA responses.

We finally determined whether the protein kinase effects were caused by changes in the activation kinetics of GABA<sub>A</sub> receptors. We operationally estimated  $EC_{50}$  and  $I_{max}^R$ , the relative maximal current, from two GABA responses (5  $\mu$ M; 2 and 14 min) and from a saturating GABA response (see *Materials and Methods*). As illustrated in Fig. 4B, the  $EC_{50}$  estimated for 21 control cells was  $5.60 \pm 0.46$   $\mu$ M, i.e., very similar to the average value of  $\approx 5$   $\mu$ M obtained from the conventional dose-response curves (Fig. 1B).  $I_{max}^R$  was also very stable at  $1.13 \pm 0.08$  after 14 min of recording (Fig. 4C). Having validated our approach, we applied it to examining the effects of 100  $\mu$ M cAMP and 100 nM PMA to respectively reduce ( $I/I_C = 0.29 \pm 0.05$ ;  $n = 11$  granule cells) or enhance ( $I/I_C = 1.92 \pm 0.35$ ;  $n = 4$  M/T cells) GABA responses (Fig. 4A). After 14 min of recording, the  $EC_{50}$  for GABA was shifted by cAMP from 5  $\mu$ M to  $12.0 \pm 2.1$   $\mu$ M (Fig. 4B). At the same time,  $I_{max}^R$  was reduced to  $0.52 \pm 0.03$  (Fig. 4C). With PMA, the  $EC_{50}$  was changed to  $3.3 \pm 0.5$   $\mu$ M (Fig. 4B).  $I_{max}^R$  was slightly increased to  $1.40 \pm 0.41$ , a value not significantly different from control cells (Fig. 4C). Thus, PKA decreases GABA<sub>A</sub> receptor function in granule cells by reducing both its affinity and maximal response amplitude. The facilitation of GABAergic function of M/T cells via PKC activation appears to be primarily caused by enhanced GABA<sub>A</sub> receptor affinity.

## DISCUSSION

Our results show that, similar to retinal amacrine cells (17), olfactory-bulb neurons exhibit stable GABA<sub>A</sub> responses. The lack of run-down despite the absence of ATP/GTP in the pipette indicates that the GABA<sub>A</sub> receptors expressed in retina and olfactory bulb are different from the isoform present in hippocampal cells (28). D1 receptors down-

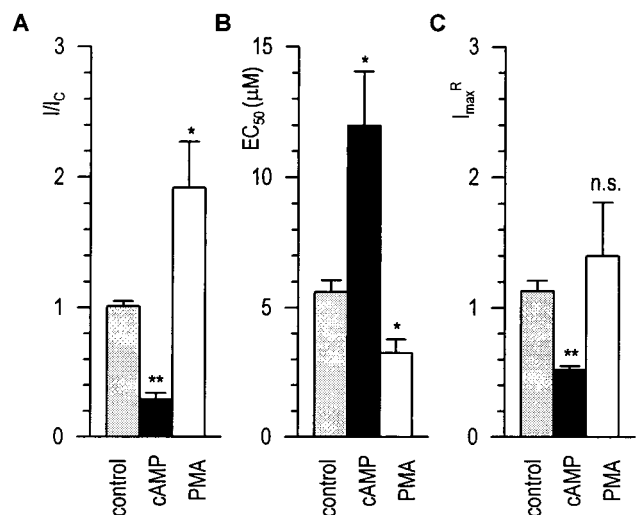


**Fig. 4.** Effects of PKA and PKC on the activation properties of GABA<sub>A</sub> receptors.  $I/I_C$  (A),  $EC_{50}$  (B), and  $I_{max}^R$  (C) determined after 14 min of whole-cell recording (see *Materials and Methods*). Average data are plotted for control (shaded bars,  $n = 21$ ), granule (100  $\mu$ M cAMP, filled bars,  $n = 11$ ), and M/T cells (100 nM PMA, open bars,  $n = 4$ ). \*\*,  $P \leq 0.01$ ; \*,  $P \leq 0.05$ .

modulate the GABA<sub>A</sub> receptor in granule cells via a PKA cascade, whereas the GABA receptor is up-modulated in M/T cells via D2 receptors and the PKC system. Both phosphorylating and dephosphorylating agents were active in our experiments, implying that the physiological steady-state of phosphorylated and nonphosphorylated GABA<sub>A</sub> receptor populations can be controlled by ambient or synaptically released dopamine.

The differential modulatory effects of dopamine on olfactory bulb GABA<sub>A</sub> receptors may be reflected in the differential distribution of D1 and D2 receptor subtypes in the internal granular/plexiform and the glomerular/external plexiform layers (22, 23), respectively. D1 and D2 receptors coupled to, respectively, adenylate cyclase in granule cells and phospholipase C in M/T cells (Figs. 2H and 3E). There is evidence that different subunits and/or consensus sites of the GABA<sub>A</sub> receptor are targeted by PKA and PKC (15, 16, 29). We have shown that the action of dopamine is to decrease the affinity of GABA<sub>A</sub> receptors in granule cells, however associated with a reduction of the maximal current response. The latter effect might arise from internalization of GABA<sub>A</sub> receptors subsequent to activation of the PKA cascade. Dopamine enhanced the GABA responses in M/T cells by increasing GABA<sub>A</sub> receptor affinity without affecting I<sub>max</sub> significantly. It is very likely that the changes in apparent GABA<sub>A</sub> receptor affinity are caused by changes in the open probability of GABA<sub>A</sub> receptor channels, as observed in retinal amacrine cells (17).

A physiological role for dopamine has been demonstrated in the olfactory bulb, where dopamine suppresses the electrical activity of mitral cells (30). Our work suggests that a more specific function of dopamine would be to fine tune GABAergic inhibition in olfactory pathways. Dopamine is highly enriched in the rat olfactory bulb and it colocalizes with GABA in a large number of neurons in the glomerular and external plexiform layers (20, 21). After corelease with GABA, dopamine could exert considerable control at two important points of olfactory signal processing, the input and output elements of M/T cells. The most significant impact is expected within the glomeruli at the synaptic triad, where GABAergic and dopaminergic periglomerular-cell dendrites control the input of M/T-cell dendrites from receptor-cell axons. It is conceivable that dopamine, acting at the D2 receptor subtype, could sharpen the molecular receptive range of odorants detected by the subset of sensory neurons that project to a single glomerulum (26, 31, 31).

Granule cells control the output of M/T cells at reciprocal dendrodendritic synapses. As lateral GABAergic inhibition is essential for odor-contrast enhancement between mitral cells, dopamine D1 receptors on granule cells could play a role in the discrimination of odorants by adjacent glomeruli (26, 33).

Dopamine receptors are involved with various forms of olfactory learning. Post-training D1 receptor blockade leads to impaired odor conditioning in neonatal rats (34). Likewise, odor-detection performance of adult animals is reduced on administering a D2 agonist (35). It is tempting to speculate that dopamine affects the synchronization of neural assemblies by modulating GABAergic inhibition and thus controls odotopic memory (36, 37).

We thank Harald Bartel for designing the drug-application system, Dr. Kurt Gottmann for help with the cell cultures, and Dr. Jack Benson for helpful comments on the manuscript. This work was supported by the Deutsche Forschungsgemeinschaft and the Fonds der Chemischen Industrie.

1. Sivilotti, L. & Nistri, A. (1991) *Prog. Neurobiol.* **36**, 35–92.
2. Bormann, J., Hamill, O. P. & Sakmann, B. (1987) *J. Physiol. (London)* **385**, 243–286.
3. Bormann, J. (1988) *Trends Neurosci.* **11**, 112–116.
4. Macdonald, R. L. & Olsen, R. W. (1994) *Annu. Rev. Neurosci.* **17**, 569–602.
5. Costa, E. (1998) *Annu. Rev. Pharmacol. Toxicol.* **38**, 321–350.
6. Bowery, N. G. (1989) *Trends Pharmacol. Sci.* **10**, 401–407.
7. Kaupmann, K., Huggel, K., Heid, J., Flor, P. J., Bischoff, S., Mickel, S. J., McMaster, G., Angst, C., Bittiger, H., Froestl, W. & Bettler, B. (1997) *Nature (London)* **386**, 239–246.
8. Polenzani, L., Woodward, R. M. & Miledi, R. (1991) *Proc. Natl. Acad. Sci. USA* **88**, 4318–4322.
9. Feigenspan, A., Wässle, H. & Bormann, J. (1993) *Nature (London)* **361**, 159–162.
10. Qian, H. & Dowling, J. E. (1993) *Nature (London)* **361**, 162–164.
11. Bormann, J. & Feigenspan, A. (1995) *Trends Neurosci.* **18**, 515–519.
12. McKernan, R. M. & Whiting, P. J. (1996) *Trends Neurosci.* **19**, 139–143.
13. Sieghart, W. (1995) *Pharmacol. Rev.* **47**, 181–234.
14. Schofield, P. R., Darlison, M. G., Fujita, N., Burt, D. R., Stephenson, F. A., Rodriguez, H., Rhee, L. M., Ramachandran, J., Reale, V., Glencorse, T. A., *et al.* (1987) *Nature (London)* **328**, 221–227.
15. Leidenheimer, N. J., Browning, M. D. & Harris, R. A. (1991) *Trends Pharmacol. Sci.* **12**, 84–87.
16. Levitan, I. B. (1994) *Annu. Rev. Physiol.* **56**, 193–212.
17. Feigenspan, A. & Bormann, J. (1994) *Proc. Natl. Acad. Sci. USA* **91**, 10893–10897.
18. Veruki, M. L. & Yeh, H. H. (1994) *Visual Neurosci.* **11**, 899–908.
19. Krishek, B. J., Xie, X., Blackstone, C., Haganir, R. L., Moss, S. J. & Smart, T. G. (1994) *Neuron* **12**, 1081–1095.
20. Mugnaini, E., Oertel, W. H. & Wouterlood, F. F. (1984) *Neurosci. Lett.* **47**, 221–226.
21. Gall, C. M., Hendry, S. H., Seroogy, K. B., Jones, E. G. & Haycock, J. W. (1987) *J. Comp. Neurol.* **266**, 307–318.
22. Levey, A. I., Hersch, S. M., Rye, D. B., Sunahara, R. K., Niznik, H. B., Kitt, C. A., Price, D. L., Maggio, R., Brann, M. R. & Ciliax, B. J. (1993) *Proc. Natl. Acad. Sci. USA* **90**, 8861–8865.
23. Coronas, V., Srivastava, L. K., Liang, J. J., Jourdan, F. & Moyse, E. (1997) *J. Chem. Neuroanat.* **12**, 243–257.
24. Bufler, J., Zufall, F., Franke, C. & Hatt, H. (1992) *J. Comp. Physiol. A* **170**, 153–159.
25. Trombley, P. Q. & Shepherd, G. M. (1994) *J. Neurophysiol.* **71**, 761–767.
26. Shepherd, G. M. (1998) *The Synaptic Organization of the Brain*, (Oxford Univ. Press, New York), 4th Ed.
27. Hamill, O. P., Marty, A., Neher, E., Sakmann, B. & Sigworth, F. J. (1981) *Pflügers Arch.* **391**, 85–100.
28. Stelzer, A., Kay, A. R. & Wong, R. K. (1988) *Science* **241**, 339–341.
29. McDonald, B. J., Amato, A., Conolly, C. N., Benke, D., Moss, S. J. & Smart, T. G. (1998) *Nat. Neurosci.* **1**, 23–28.
30. Duchamp-Viret, P., Coronas, V., Delaleu, J.-C., Moyse, E. & Duchamp, A. (1997) *Neuroscience* **79**, 203–216.
31. Hildebrand, J. G. & Shepherd, G. M. (1997) *Annu. Rev. Neurosci.* **20**, 595–631.
32. Mori, K. & Yoshihara, Y. (1995) *Prog. Neurobiol.* **45**, 585–619.
33. Yokoi, M., Mori, K. & Nakanishi, S. (1995) *Proc. Natl. Acad. Sci. USA* **92**, 3371–3375.
34. Weldon, D. A., Travis, M. L. & Kennedy, D. A. (1991) *Behav. Neurosci.* **105**, 450–458.
35. Doty, R. & Risser, J. M. (1989) *Psychopharmacology* **98**, 310–315.
36. Ritz, R. & Sejnowsky, T. J. (1997) *Curr. Opin. Neurobiol.* **7**, 536–546.
37. Stopfer, M., Bhagavan, S., Smith, B. H. & Laurent, G. (1997) *Nature (London)* **390**, 70–74.